

Ultrasonic attenuation in single crystals of dilute Zn-Mn alloys*

D. Y. Lou[†] and H. E. Bömmel[‡]

University of California at Los Angeles, Los Angeles, California 90024

(Received 12 October 1973)

Although theoretical calculations on the electronic transport properties of superconductors doped with magnetic impurities have existed for a long time, no experimental work has yet been done. We have studied the ultrasonic attenuation of Zn doped with Mn in both the normal and the superconducting state by conventional pulse-echo techniques. The longitudinal-wave attenuation was measured at 25 MHz along both the [0001] and the [1010] axis. The transverse-wave attenuation was measured at 20 MHz along the [1010] axis with polarization along the [0001] axis. Impurity concentrations n_i from $0.05n_{cr}$ to $0.64n_{cr}$ were used. Calculations made by Snow on the basis of the Abrikosov-Gorkov model were used to fit the experimental data, with good results. The conclusion is that in the temperature and concentration regime studied the simple Abrikosov-Gorkov model is sufficient to explain the transport as measured by ultrasonic attenuation.

I. THEORY

A. Gapless superconductivity

Bardeen, Cooper, and Schrieffer (BCS) explained the phenomenon of superconductivity by showing that, in the presence of an attractive interaction V , two electrons can form a bound state beneath the Fermi surface. The electrons which are thus paired are the time-reversed states \vec{p}' , $-\vec{p}'$. In collisions with nonmagnetic impurities, time-reversal invariance is preserved, provided that we characterize (\vec{p}, \vec{s}) as eigenstates of the impure Hamiltonian, and the Cooper pairs are not broken up. These pairs then have an infinite lifetime. Thus the properties of a superconductor are only slightly influenced by the presence of nonmagnetic impurities. In the presence of magnetic impurities, Matthias, Suhl, and Corenzwit¹ have shown that the critical temperature T_c is depressed significantly and that the relevant interaction is the spin-dependent perturbation Hamiltonian $J\vec{S}_e \cdot \vec{S}_i$. Here J is the exchange interaction, typically of the order of 0.1 eV for transition elements and 0.01 eV for rare earths. This interaction is not invariant under time reversal, acting oppositely on the opposite spins, and thus the \vec{p}' , $-\vec{p}'$ states will be broken up by collision. The paired states will then have a finite lifetime τ_s . This gives an energy spread $\Gamma_s = \hbar/\tau_s$ and states are introduced into the energy gap.

A new theory for superconductors doped with magnetic impurities was therefore proposed by Abrikosov and Gorkov.² This theory is based on the model of randomly oriented independent localized impurity spins coupled weakly to the conduction electrons via the exchange interaction. Extensive calculations have been made on the basis of this model.³ The major results of this theory are that, with the addition of magnetic impurities,

the infinite peak in the BCS density of states is smeared out, and the energy gap E_g is narrowed. E_g no longer corresponds to the order parameter Δ . E_g is depressed faster than T_c . For any impurity concentration n_i , there is always a gapless region just below T_c and the superconductor is completely gapless when the pair-breaking lifetime $\Gamma_s = \Delta_p(0)(n_i/2n_{cr}) = \Delta(T, \Gamma_s)$. This corresponds to an impurity concentration n_i so that $l_e \approx \xi$ and long-range ordering of the electrons is destroyed. Short-range ordering, however, is still preserved; $\Delta \neq 0$ and the superconductor can still carry supercurrent.

Direct measurements of the energy gap have been made on quenched-evaporated thin films by tunneling⁴ and far-infrared⁵ experiments. Agreement was good for rare earths, but poor for transition metals, due perhaps to the breakdown of the weak-scattering assumption.

A wide variety of other mechanisms has been shown to produce depairing, with corresponding alteration of the energy spectrum of the quasiparticles. For example, magnetic fields,⁶ currents in thin films,⁷ magnetic fields in type-II superconductors,⁸ and proximity to normal metals^{9,10} all appear to have somewhat similar effects on the electron-energy spectrum in various limits.

B. Ultrasonic attenuation

Although theoretical calculations on the electronic transport properties of superconductors have existed for a long time,¹¹⁻¹⁵ no experimental work has yet been done. We have investigated these properties by ultrasonic-attenuation measurements for typical experimental conditions $\Gamma_n \gg \Gamma_s$, $\Gamma_n \gg \Delta$, and $ql_e \ll 1$. Here Γ_n is the scattering lifetime from nonmagnetic impurities, Γ_s is the scattering lifetime for magnetic impurities, Δ is the order parameter, q is the phonon wave vector, and l_e is the electronic mean free path.

Snow¹⁴ obtained the following results for longitudinal waves:

$$\frac{\alpha_s}{\alpha_n} = \frac{1}{\bar{\omega}} \int_{-\infty}^{\infty} [f(\omega) - f(\omega + \bar{\omega})] \times [N(\omega)N(\omega + \bar{\omega})C(\omega, \bar{\omega})] d\omega \quad (1)$$

or

$$\begin{aligned} (\alpha_s/\alpha_n) &= (\alpha_s/\alpha_n)_{QP} + (\alpha_s/\alpha_n)_{DP} \quad , \\ \left(\frac{\alpha_s}{\alpha_n}\right)_{QP} &= \frac{2}{\bar{\omega}} \int_{\omega_f}^{\infty} d\omega [N(\omega)N(\omega + \bar{\omega})C(\omega, \bar{\omega})] \\ &\quad \times [1 - 2f(\omega + \bar{\omega})] \quad , \quad (2) \\ \left(\frac{\alpha_s}{\alpha_n}\right)_{DP} &= \frac{1}{\bar{\omega}} \int_{\omega_f - \bar{\omega}}^{\omega_f} d\omega [N(\omega)N(\omega + \bar{\omega})C(\omega, \bar{\omega})] \\ &\quad \times [1 - 2f(\omega + \bar{\omega})] \quad , \end{aligned}$$

where the subscript QP denotes the contribution from the excitation of quasiparticles by the phonons and the subscript DP denotes the contribution from the depairing of the Cooper pairs by the phonons:

$$N(\omega) = \text{Im} \{u(\omega)/[1 - u^2(\omega)]^{1/2}\} \quad (3)$$

is the density of states of quasiparticles,

$$P(\omega) = \text{Im} \{1/[1 - u^2(\omega)]^{1/2}\}$$

is the density of states of pair excitation,

$$C(\omega, \bar{\omega}) = 1 - \frac{\omega(\omega + \bar{\omega})}{\Delta^2 |u(\omega)|^2 |u(\omega + \bar{\omega})|^2}$$

is a generalization of the BCS coherence factor, and $u(z)$ is the characteristic function of the Abrikosov-Gorkov theory, which satisfies the Abrikosov-Gorkov equation

$$\frac{z}{\Delta} = u(z) \left(1 - \frac{i\Gamma_s/\Delta}{[u^2(z) - 1]^{1/2}} \right) \quad (4)$$

Similarly, Kadanoff and Falko have shown that the attenuation for transverse waves in the limit of $\alpha_n \gg \alpha_s$, $\alpha_n \gg \Delta$, and $ql_e \ll 1$ is given by

$$(\alpha_s/\alpha_n)_T = g(ql)(\alpha_s/\alpha_n)_L \quad , \quad (5)$$

where

$$g(a) = \frac{3}{2a^2} \left(\frac{a^2 + 1}{a} \arctan a - 1 \right) \quad .$$

For $ql \ll 1$, $g(ql) \approx 1$ and

$$(\alpha_s/\alpha_n)_T = (\alpha_s/\alpha_n)_L \quad (6)$$

(Ref. 13).

II. EXPERIMENTS

A. General considerations

It is well known that magnetic impurities have an aversion to solution in superconductors. This

is why Woolf and Reif⁴ used the quenched-evaporated-film technique. For ultrasonics work we need impurities in homogeneous solution in single crystals. The simplest such system appears to be the transition metals Mn and Cr in Zn. Boato, Bugo, and Rizzuto¹⁶ and Boato, Gallinaro, and Rizzuto¹⁷ have studied the properties of these systems. It was found that n_{cr} for Mn in Zn is 25 ppm, and for Cr in Zn, 45 ppm. For ease of preparation the Zn-Mn system was chosen.

B. Sample preparation

The solubility of Mn in Zn is approximately 0.5 at.% at the eutectic (420 °C) and decreases rapidly as temperature is lowered.¹⁸ In order to maintain a reasonable accuracy in Mn concentration in the preparation of 10-ppm Zn-Mn alloys, the following procedure was adopted. We took 99.999+%-pure mossy Zn pieces, etched off the surface-oxide layer with dilute nitric acid, and melted them together in a constricted Pyrex-glass container under 10⁻⁶-Torr vacuum in an induction furnace. Whatever dirt was originally in the Zn would tend to float and stay above the constriction. The container was then sealed and the Zn zone refined several times. This Zn was analyzed by Pacific Spectrochemical Laboratory for impurity content. The results are shown in Table I.

We then took approximately 20 g of this Zn, mixed it with approximately 60 mg of 99.99%-pure Mn powder which had been outgassed under 10⁻⁶-Torr vacuum in an induction furnace at 500 °C for approximately 10 h, and melted the two together in a Pyrex crucible. The melt was then sealed off and stirred constantly at a temperature of 500 °C overnight, and then quenched while being stirred. This gave us a stock piece of nominally 0.3-wt% Mn in Zn. The stock piece was cut into three sections by a wire saw with silicon-carbide grit. The top and bottom pieces were analyzed spectrochemically and by neutron-activation analysis. The results of neutron-activation analysis are shown in

TABLE I. Impurities content of the pure Zn used as starting material as measured by Pacific Spectrochemical Laboratory.^a

Zn	Remainder
Mg	4.0 ppm
Cu	1.5 ppm
Cd	Trace
Pb	Trace
Si	34 ppm

^aThe analysis is semiquantitative. Relative concentrations between two samples are accurate to 5%. Absolute concentrations may be as far off at 50%. Non-metallic elements are not detected.

TABLE II. Homogeneity analysis of Zn-Mn stock piece *B*.

	Bottom	Top
Mn	0.390 at. %	0.403 at. %

Table II. The middle section was used for crystal preparation.

To prepare crystals of the order of 10-ppm Mn in Zn, we diluted the stock piece by mixing approximately 20 g of Zn as prepared above with the proper weight of the stock piece. Single crystals were grown by standard Bridgman technique under a high-purity argon atmosphere in a Pyrex crucible. The crystals obtained were annealed at 120 °C for 8 h. They had a diameter of approximately 0.5 in. and a length of 1.0 in. In order to propagate pure acoustic modes in a crystal, it is necessary to orient accurately the crystal along a specific crystal axis. For these experiments, the crystals were first cleaved along the *c* plane and then accurately oriented by means of back reflection Laue x-ray photographs.

After x-ray orientation, the crystals were cut into convenient lengths (about 0.5 in. long) with a diamond saw. Extreme care has to be taken to minimize damage to the crystal surface and interior. Conventional spark-erosion cutting was not possible because the sparks tend to go in between the *c* planes and crack the crystal. The two faces were cut as parallel as possible, then ground flat using a Crane Packing Co. Lapmaster 12 with the size 1800 aluminum-oxide abrasive, and then ground by hand using 32-mesh aluminum-oxide grit on nylon cloth. This procedure produced crystals flat to within 0.000 010 in., as measured by a Davidson Optronics Model No. D 309 Interferometer (one fringe of green light). The quality of the crystals thus produced were judged acceptable by the excellent ultrasonic-pulse-echo pattern produced.

C. Measurement techniques

Conventional pulse-echo techniques with superheterodyne detection were used, augmented by a boxcar integrator,¹⁹ which improved the accuracy to 0.02 dB (Fig. 1). Triggering pulses were obtained from a sync and delay unit to trigger a Tektronix No. 535A oscilloscope, a Madison Industries No. PR-20-290 rf pulser, a Hewlett-Packard No. 608D VHF generator to generate the comparison pulse and two General Radio No. 121B pulsers to generate the necessary delay for the gating pulses for the boxcar. Tuning to the sample was achieved by using coaxial cables of proper length. The echoes from the sample, together

with the comparison pulse, were beat against a continuous wave from a local oscillator in a mixer and sent to a 10-MHz i.f. strip. Because the boxcar integrator can take only inputs of ± 10 V and does not amplify, this signal was first amplified by a Tektronix No. 1A1 dual-trace plug in, so that later echoes presented a large enough signal; it was then voltage limited by a Zener diode, so that the earlier echoes did not overload the boxcar input amplifier and was then fed into the boxcar integrator. The boxcar was operated in the differential mode. The echoes signal was referenced to a standard signal supplied by the Hewlett-Packard No. 608D VHF signal generator and attenuated by an Empire Device Products Corp. No. AF-106-F precision step attenuator. Signals of the order of 0.1 dB were measured by making the necessary correction in the step attenuator to bring the boxcar output back into balance. Signals of less than 0.1 dB were interpolated from the boxcar output.

Pure Zn superconducts at 0.87 °K. Doping of Mn in Zn depresses T_c further. Thus we are only interested in temperatures below 1.4 °K. Temperatures between 0.4 and 1.4 °K were obtained with a standard He³ system. Temperatures between 0.5 and 0.1 °K were obtained with a standard adiabatic demagnetization system.²⁰ Temperature was measured with a CryoCal Inc. No. CR-50-He³-VC germanium-resistance thermometer. Two of these resistors were bought uncalibrated. They were calibrated against He⁴ vapor pressure from 4.2 to 1.4 °K, He³ vapor pressure as measured by

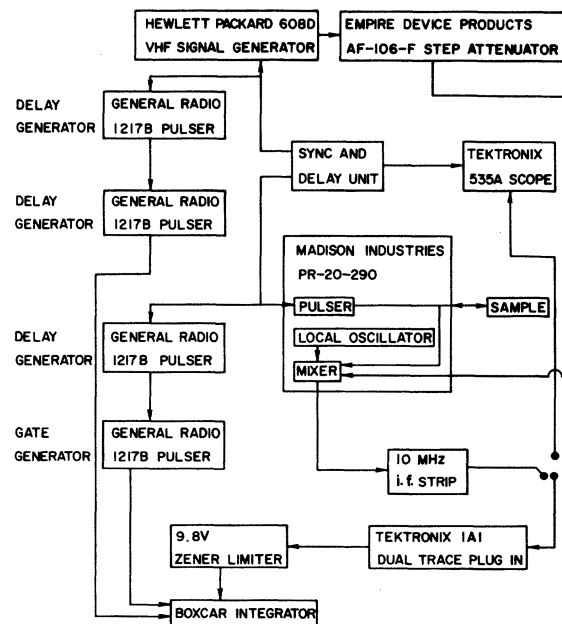


FIG. 1. Electronic equipment.

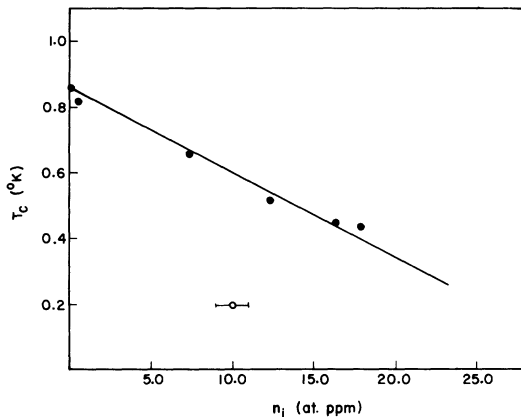


FIG. 2. Plot of the transition temperature T_c as measured by ultrasonic attenuation versus the amount of Mn impurities doped in n_i . The uncertainty in T_c measurement is taken to be $\pm 10\%$.

a McLeod gauge, corrected for thermomolecular effects²⁰ from 1.4 to 0.4 °K, and with a cerium magnesium nitrate magnetic-susceptibility thermometer at the University of Southern California from 0.6 to 60 m °K. Two-terminal resistance measurements were made by an ac resistance bridge with phase-sensitive detection. We believe that the measurements are accurate to $\pm 1\%$.

III. RESULTS

A. Introduction

We found that, contrary to published reports²¹ Zn does tend to grow along the [0001] axis if the

crucible tip is pulled properly (i. e., symmetrically). However, the [10 $\bar{1}$ 0] axis was chosen for these experiments since the electronic attenuation for acoustic waves traveling along the [0001] axis is so high that no echoes at liquid-helium temperatures have ever been reported for Zn in the normal state. This is generally attributed to the abnormal anisotropy of the Zn Fermi surface.²²

Minimal doping with magnetic impurities apparently changes the electronic mean free path sufficiently to produce observable echoes.

Three sets of experiments were performed: 25-MHz longitudinal waves along the [10 $\bar{1}$ 0] axis, 25-MHz longitudinal waves along the [0001] axis, and 20-MHz transverse waves along the [10 $\bar{1}$ 0] axis polarized along the [0001] direction. These frequencies give $h\nu/\Delta_p(0) \approx 10^{-5}$ and are believed to satisfy the low-frequency limit of the theory. The frequency dependence of the attenuation was not pursued because it was discovered that, even at 50 MHz, the attenuation became so high that the echoes were barely detectable.

B. Numerical calculations

The algorithm used by Snow¹⁴ was adopted for calculation. We have

$$\frac{\alpha_s}{\Delta(T, \alpha_s)} = \frac{n_i}{n_{cr}} \frac{\Delta_p(0)}{2\Delta(T)} \quad (7)$$

The Abrikosov-Gorkov equation (4) can be solved by the substitution $u = \cosh(x + iy)$ to obtain the pair of equations

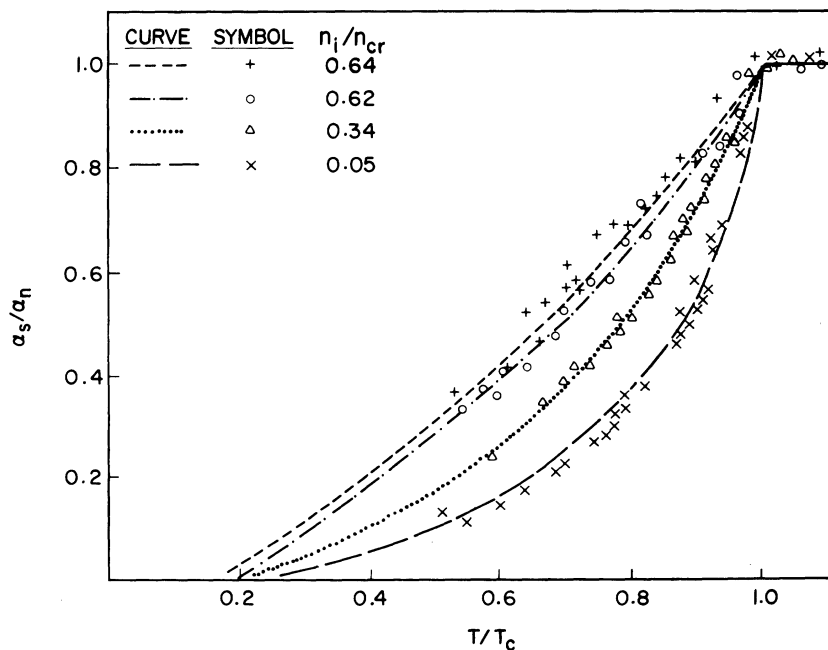


FIG. 3. Selected data of normalized attenuation α_s/α_n versus reduced temperature T/T_c for 25-MHz longitudinal waves along the [10 $\bar{1}$ 0] axis.

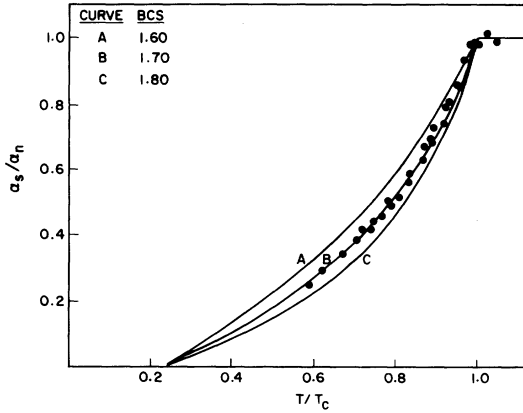


FIG. 4. Plot of the normalized attenuation α_s/α_n versus reduced temperature T/T_c for various values of the BCS constant for the experimental data of Fig. 3, to show the range of BCS values that will fit the experimental data.

$$\sin^3(2y) + (\Omega^2 + \alpha^2 - 1) \sin(2y) - 2\Omega\alpha = 0, \quad (8)$$

$$\cosh x \cos(2y) = \Omega \cos y - \alpha \sin y,$$

where

$$\Omega = \frac{\bar{\omega}}{\Delta(T, \Gamma_s)}, \quad \alpha = \frac{\Gamma_s}{\Delta(T, \Gamma_s)}.$$

The cubic equation can be written $\xi^3 + p\xi + q = 0$, with $\xi = \sin(2y)$. When $D = -4p^3 - 27q^2 < 0$,

$$\xi = z - p/3z, \quad z = \left(-\frac{q}{2} + \frac{(3D)^{1/2}}{18} \right)^{1/3},$$

and when $D \geq 0$,

$$\xi = k \cos A, \quad A = \frac{1}{3} \arccos(-4q/k^3), \quad k = \left(-\frac{4}{3}p \right)^{1/2},$$

and

$$N(\omega) = \sinh(2x) / [\cosh(2x) - \cos(2y)],$$

$$|u(\omega)|^2 = 0.5 [\cosh(2x) + \cos(2y)].$$

Equation (2) was then integrated numerically by Simpson's rule to obtain $(\alpha_s/\alpha_n)_{QP}$ and $(\alpha_s/\alpha_n)_{DP}$. It was found that the integrand has a singularity when the phonon frequency $\bar{\omega} = 0$. Consequently we set $\bar{\omega} = 20\text{--}30$ MHz as prescribed by experimental conditions, we must set $(\alpha_s/\alpha_n)_{DP} = 0$. The curves of $(\alpha_s/\alpha_n) = (\alpha_s/\alpha_n)_{QP}$ computed this way agree well with those obtained by Griffin and Ambegaokar,¹² and are the theoretical curves used to fit the experimental data.

C. Experimental results

Figures 2–6 show the results of the experiments. The data are plotted in terms of reduced attenuation α_s/α_n versus reduced temperature T/T_c . It is easy to determine T_c from the point at which the attenuation drops off rapidly. From T_c/T_{cP} we obtain n_i/n_{cr} from Ref. 14. The accuracy of determining n_i/n_{cr} by this technique is limited only by the accuracy of the temperature measurement, which we believe to be better than $\pm 1\%$. The ratios of n_i/n_{cr} thus obtained agree well with the n_i 's obtained from measuring the weight of the impurities doped in (Fig. 2). The experimental data for the attenuation of longitudinal waves along $[10\bar{1}0]$ axis are then fitted to the numerical calculations developed in Sec. IIIB with a constant residual at-

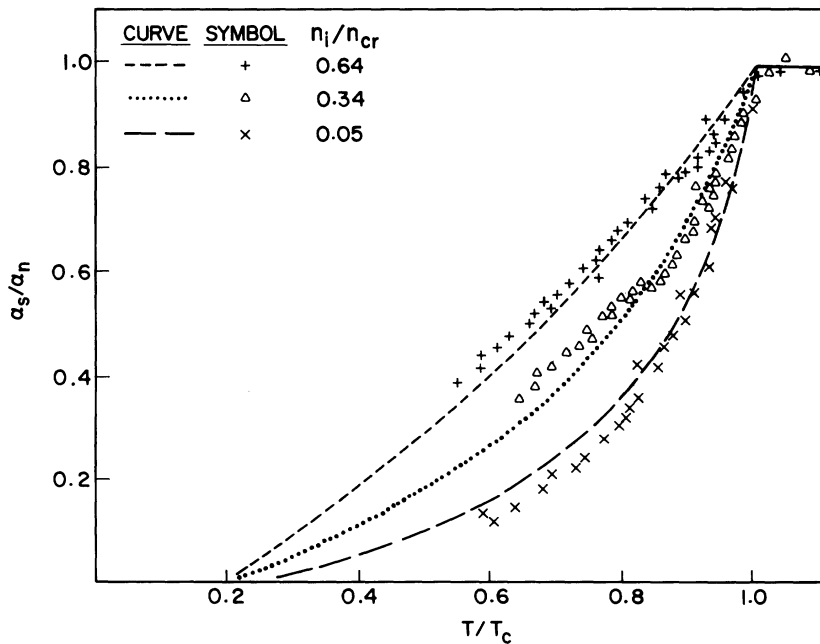


FIG. 5. Selected data of normalized attenuation α_s/α_n versus reduced temperature T/T_c for 20-MHz transverse waves polarized along the $[0001]$ axis propagating along the $[10\bar{1}0]$ direction.

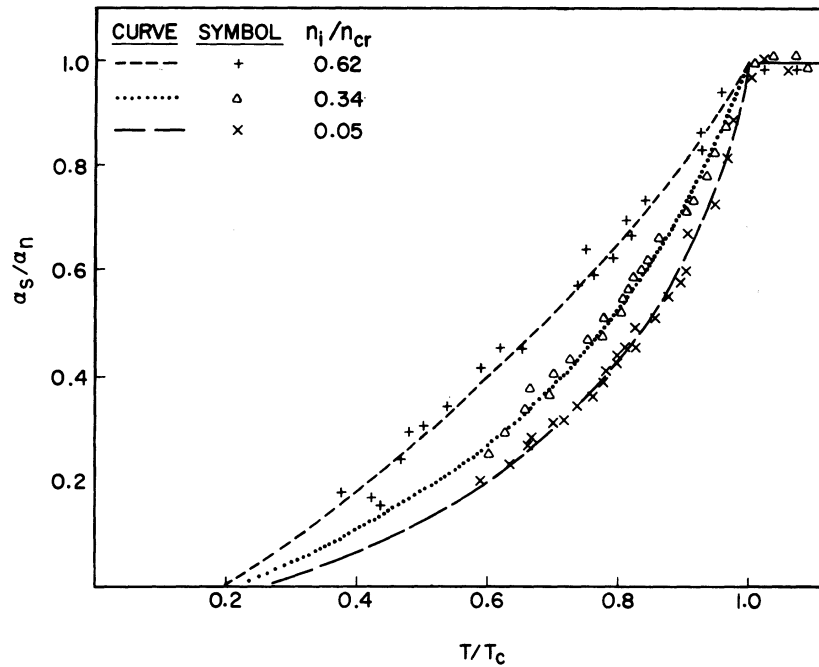


FIG. 6. Selected data of normalized attenuation α_s/α_n versus reduced temperature T/T_c for 25-MHz longitudinal waves along the [0001] axis.

tenuation α_r , and the BCS constant $\Delta(0, \alpha_s)/k_B T_c(\alpha_s)$ as parameters. The results are plotted in Fig. 3.

Figure 4 shows the difference in fit to experimental data for different values of the BCS constant at a low-impurity concentration. The theoretical curves computed above prove to be rather insensitive to changes in the value of the BCS constant at the higher concentrations. For example, at $n_i = 0.6n_{cr}$ all values of the BCS constant from $\Delta = 1.50k_B T_c$ to $\Delta = 1.86k_B T_c$ generate essentially the same theoretical curve. It was thus impossible to study the effect of magnetic impurities on this constant. Thus we claim the accuracy of the value of the BCS constant extracted from these experiments to be ± 0.1 at low concentrations and at most ± 0.2 at higher concentrations.

Figure 5 shows the data for the transverse wave attenuation. Here we take the values of n_i/n_{cr} and BCS constant as obtained in the longitudinal-wave measurements, and fit the experimental data with a constant residual attenuation α_r . For the sample with the lowest concentration of impurities $n_i = 0.05n_{cr}$, we find the commonly observed discontinuous drop for pure samples at the critical temperature T_c . The data were fitted to the theoretical curve after the discontinuous drop has been taken out.

This discontinuous drop broadens out and eventually vanishes as the concentration of impurities is increased, and this behavior may possibly account for the loss of fit for the transverse waves in the sample with higher concentrations, since data for these samples were fitted without includ-

ing this rapid drop behavior.

The results for the [0001] axis are shown in Fig. 6. Here the n_i/n_{cr} data are taken from previous measurements, while the BCS constant is used together with a constant residual attenuation α_r as fitting parameters.

In order to fit the data, we have to change the BCS constant from 1.50 ± 0.05 to 1.70 ± 0.10 along the [0001] axis on increasing the doping from $n_i = 0.05n_{cr}$ to $n_i = 0.34n_{cr}$. This means there is a smearing out of the anisotropy in the energy gap as the impurity concentration is increased. This is consistent with Anderson's theorem for non-magnetic impurities in superconductors.¹

We see that it is possible to fit quite well the experimental data with the theoretical calculations based on the simple Abrikosov-Gorkov model. This is somewhat different from the results of Reif's group on tunneling⁴ and far-infrared absorption⁵ in thin films. Whereas the thin-film experiments were done with Mn concentrations of the order of 0.1 at. % and Gd concentrations of the order of 1 at. %, experiments here are done with Mn concentrations of the order of 10 at. ppm. Our results are consistent with their results in the sense that the far-infrared data did show that the discrepancies with the Abrikosov-Gorkov theory become less pronounced with decreasing Mn concentrations.

It is not clear why there should be such concentration-dependent discrepancies. The most obvious explanation would be that at the higher concentrations, the Mn atoms are interacting, for

example, via the Ruderman-Kittel-Kasuya-Yoshida interaction. Susceptibility measurements of Hirschhoff, Symko, and Wheatley²³ have shown that for 10-ppm Mn in Cu, the magnetic ordering temperature is less than 10 m°K. We can, therefore, probably assume that for 10-ppm Mn in Zn at 0.2°K, the impurity's spins are noninteracting. On the other hand, susceptibility measurements by Korn²⁴ show that for 0.07 at. % of Mn in Pb ($T_c/T_{c0} \approx 0.9$), the spin-ordering temperature is approximately 0.2°K. Thus we certainly must accept the presence of interacting spins in the tunneling experiments, and the possibility of the presence of

interacting spins in the far-infrared experiments. This may explain why the Abrikosov-Gorkov theory failed to fit the thin film data obtained by Reif's group, but was sufficient for our ultrasonic-attenuation data.

ACKNOWLEDGMENTS

We would like to acknowledge the extensive help extended to us by Dr. E. Chock in sample preparation. We would also like to acknowledge the technical assistance rendered by K. Stolt and F. Lacy and several helpful discussions with Dr. N. Rivier, Dr. F. Ferguson, and Dr. W. G. Clark.

*Work supported in part by National Science Foundation Grant No. GP8167.

†Present address: Bell Laboratories, Murray Hill, N. J. 07974.

‡Present address: Physics Dept., Universität Konstanz, Konstanz, Germany.

¹B. T. Matthias, H. Suhl, and E. Corenzwit, *Phys. Rev. Lett.* **1**, 93 (1958).

²A. A. Abrikosov and L. P. Gorkov, *Zh. Eksp. Teor. Fiz.* **39**, 1781 (1960) [*Sov. Phys.-JETP* **12**, 1243 (1961)].

³S. Skalski, O. Betbeder-Matibet, and P. R. Weiss, *Phys. Rev.* **136**, A1500 (1964).

⁴M. A. Woolf and F. Reif, *Phys. Rev.* **137**, A557 (1965).

⁵G. J. Dick and F. Reif, *Phys. Rev.* **181**, 774 (1969).

⁶K. Maki, *Prog. Theor. Phys.* **31**, 731 (1964).

⁷K. Maki, *Prog. Theor. Phys.* **29**, 10 (1963); *Prog. Theor. Phys.* **29**, 333 (1963).

⁸P. G. deGennes, *Superconductivity of Metals and Alloys*, (Benjamin, New York, 1966).

⁹P. Fulde and K. Maki, *Phys. Kondens. Mater.* **5**, 380 (1966).

¹⁰P. G. deGennes, *Rev. Mod. Phys.* **36**, 225 (1964).

¹¹H. Bömmel, *Phys. Rev.* **96**, 220 (1954).

¹²A. Griffin and V. Ambegaokar, *Proceedings of the Ninth International Conference on Low Temperature Physics* (Plenum, New York, 1965), p. 524.

¹³L. P. Kadanoff and I. I. Falko, in Ref. 12, p. 378.

¹⁴J. A. Snow, *Phys. Rev.* **172**, 455 (1968).

¹⁵T. Tsuneto, *Phys. Rev.* **121**, 402 (1961).

¹⁶G. Boato, M. Bugo and C. Rizzuto, *Nuovo Cimento XLV B*, 226 (1966).

¹⁷G. Boato, G. Gallinaro, and C. Rizzuto, *Phys. Rev.* **148**, 353 (1966).

¹⁸M. Hansen and K. Anderko, *Constitution of Binary Alloys* (McGraw-Hill, New York, 1958).

¹⁹W. G. Clark and A. Kerlin, *Rev. Sci. Instrum.* **38**, 1593 (1967).

²⁰F. E. Hoare, L. C. Jackson, and N. Kurti, *Experimental Cryophysics* (Butterworth, London, 1961).

²¹J. J. Gilman, *The Art and Science of Growing Crystals* (Wiley, New York, 1963).

²²M. J. Lea and E. R. Dobbs, *Phys. Lett. A* **27**, 556 (1968).

²³E. C. Hirschhoff, O. G. Symko, and J. C. Wheatley, *Phys. Lett. A* **33**, 19 (1970).

²⁴D. Korn, *Z. Phys.* **187**, 463 (1965).